Building and Environment 46 (2011) 2657–2665

Contents lists available at ScienceDirect

Building and Environment

journal homepage: www.elsevier.com/locate/buildenv

Effect of uneven building layout on air flow and pollutant dispersion in non-uniform street canyons

Zhao-Lin Gu [a,d,*], Yun-Wei Zhang [b], Yan Cheng [a,c], Shun-Cheng Lee [c]

[a] School of Human Settlements and Civil Engineering, Xi'an Jiaotong University, China
[b] School of Energy and Power Engineering, Xi'an Jiaotong University, China
[c] Department of Civil and Structural Engineering, Hong Kong Polytechnic University, Hong Kong, China
[d] SKLLQG, Institute of Earth Environment, Chinese Academy of Sciences, China

A R T I C L E I N F O

Article history:
Received 21 January 2011
Received in revised form
26 June 2011
Accepted 29 June 2011

Keywords:
Uneven building layout
Non-uniform street canyon
LES
Air flow
Pollutant dispersion

A B S T R A C T

Uneven building layouts and non-uniform street canyons are common in actual urban morphology. To study the effects of building layouts on air flow in non-uniform street canyons, various building arrangements are designed in this study. Simulations are carried out under four cases (i.e., a uniform street canyon as Case 1 and three non-uniform canyons as Cases 2–4) with parameter change of the occupying ratio of high buildings (ORHB) in the computational domain and their bilateral allocation as well as the combinations of stepup and/or stepdown notches. In the three non-uniform canyons, stepup and stepdown notches are separating (with ORHB of 25% for Case 2 and 75% for Case 4) or adjoining (with ORHB of 50% for Case 3). The air flow and pollutant dispersion in these street canyons are investigated using Large-eddy Simulation (LES). The air flow structures in the non-uniform street canyons are more complicated than in the uniform street canyon. Inside the non-uniform street canyons, the tilting, horizontal divergence and convergence of wind streamlines are found. Large-scale air exchanges of air mass inside and above the street canyons are found as well. At the pedestrian level, the concentrations of simulated pollutants (e.g., the mean and maximum concentrations) in the non-uniform street canyons are lower than those in the uniform one, suggesting that uneven building layouts are capable of improving the dispersion of pollutants in urban area. Further studies on Case 2–4 show that the separation of stepup and stepdown notches along the street increases the wind velocities in the vicinity of high buildings, while the adjoining of stepup and stepdown notches decreases the wind velocities. Low concentrations of pollutant at the pedestrian level are found in Case 2 compared to Cases 3 and 4. Thus, the separation of stepup and stepdown notches in non-uniform street canyons might be a good choice for uneven building layout arrangements from the point of view of pollutant dispersion and human health.

1. Introduction

Street canyons are basic geometric units of urban areas, composed of buildings and streams of people and public transportation. However, poor air quality is often observed at the pedestrian level inside these street canyons since the air recirculation there will stop pollutants from dispersing to the layer aloft [1,2].

The flow pattern inside a street canyon is mainly determined by the aspect ratio (AR) free wind velocity, building roof shape, building layout, atmospheric instabilities [3–7]. AR is defined as the building height-to-street-width (H/W, where H is the building height and W is the street width). Dispersion behavior of pollutants from vehicles is closely linked to the flow pattern inside street canyons. Several methods, such as laboratory-scale experiments [6,8,9], in-situ measurements [1,10,11], and computational fluid dynamics (CFD) simulations [6,12–15] have been utilized for investigation of street canyon air flow and pollutant dispersion.

However, most previous studies, where uniform street canyon models were used, focus on the effects of free wind velocity, aspect ratio, building roof shape and urban planting. In uniform street canyon models, the buildings are assumed to be of the same height, and the effect of the layout with different height buildings is neglected. But in actual street canyons, buildings are usually of different heights. Simulation results of uniform street canyon models may produce air flow patterns much different from those in

* Corresponding author. School of Human Settlements and Civil Engineering, Xi'an Jiaotong University, China. Tel.: +86 8339 5100.
E-mail address: guzhaoln@mail.xjtu.edu.cn (Z.-L. Gu).

0360-1323/$ – see front matter © 2011 Elsevier Ltd. All rights reserved.
doi:10.1016/j.buildenv.2011.06.028

non-uniform street canyons with different high buildings. Thus, studies based on uniform street canyon models cannot reveal the effects of the building layouts of actual street canyons.

In an actual street canyon, buildings on one side of a street may usually have different heights and are asymmetric to those on the opposite side, and the street canyon presents an uneven layout. The flow patterns inside the actual street canyon are significantly affected by the uneven building layout [16]. A single high-rise building can cause wind velocity amplification in its vicinity [17], while a range of high-rise buildings can induce a compelling effects to the downwind urban areas not only on the air ventilation but also on the pollutant dispersion [18]. So study of air flow and pollutant dispersion as well as the effect of building arrangements on the air flow and pollutant dispersion in non-uniform street canyon models will help us to understand pollutant dispersion in actual street canyons and provide suggestions for urban street planning.

A few studies have already focused on non-uniform street canyons. Nelson et al. [19] measured the wind field within the Oklahoma City Park Avenue street canyon. Based on their measurements, a hypothetical flow structure inside the street canyon was hypothesized, illustrating the wind downdraft and horizontal divergence resulting from non-uniform building arrangement. With laboratory-scale experiments and numerical simulations, Baik and Park [6] investigated the flow patterns in stepup notch or stepdown notch street canyons, where unilateral buildings have the same height but the heights of buildings on the upwind side are lower (or higher) than those on the downwind side. Baik and Park's simulation of the stepdown notch flow demonstrated two counter-rotating vortices inside the street canyon. Kastner-Klein and Rotach [8] studied the wind and turbulence characteristics in an unban roughness layer in a wind tunnel model where buildings were arranged by blocks with different heights, and measured the vertical wind distributions at different points. However, they did not analyze the effects of building layouts along the street in details. Hu and Wang [17], using a CFD approach, studied the effect of single high-rise building on the street-level wind structure in a built-up area, and demonstrated the amplification of wind velocities in the vicinity of the building. However, actual street canyons are usually composed of multiple high-rise buildings, and it is necessary to investigate the interactions between the air flows and the layout of multiple high-rise buildings.

Street canyon physical models can be assigned in two categories: isolated street canyon and urban roughness street canyon [20]. The former refers to the case of open country, while the latter refers to the urban fabric. Larger computational domains are usually used in CFD simulations of air flow inside and above street canyons [17,21], especially for the isolated street canyon cases [6,22]. Grids for large computational domains are usually in rough resolutions so as to reduce computational load and ensure the execution of computing. For example, Hu and Wang used in their simulations a grid system with widths of 5 m $\times$ 5 m in longitudinal and lateral directions, and diminished only the vertical grid widths near ground surface [17]. For urban roughness street canyon cases, computational domains containing only the basic elements of the street canyons were usually selected and the periodic boundary wind conditions were used, so as to get high resolution wind velocity field and turbulent strength, and to reduce computational load as well [14,23,24]. However, for non-uniform street canyons, classical periodic boundary conditions are not suitable any more, and the boundary conditions need reconsideration.

The motivation of this work is to propose a practicable, simplified uneven street canyon model and to study effects of uneven building layout on air flow and pollutant dispersion in non-uniform street canyons.

2. Non-uniform street canyon modeling

Actual street canyons usually take on uneven building layouts, which, in urban roughness layer, result in difficulty in the modeling of a non-uniform street canyon and the formation of boundary conditions. To study the effect of non-uniform street canyon layout on air flow, different stepup and/or stepdown notch street canyons are simulated in this study. Models with a layout of different high buildings (low building height: H_1 = 30 m; high building height: H_2 = 45 m) are built for simplified non-uniform street canyons. The building heights are anticipated to be large enough to cause evident effects on air flow and pollutant dispersion in street canyons. The relative positions of opposite buildings will produce different stepup and/or stepdown notch flow patterns in the street canyons when free wind flows over the streets perpendicularly.

Fig. 1 demonstrates an urban roughness street canyon model, where free boundary-layer air flows perpendicularly to the street. The dashed lines depict the computational domain. Although the buildings are assumed in simplified layouts, which is greatly different from the actual street canyons, this model can show the building heights variations along the street. These models are anticipated to be typical and the simulated results are anticipated be universal.

The computational domain boundaries in the lateral direction, y, are set in the middle sections of the bilaterally laid buildings, as air flow patterns inside and above the street canyon can be assumed symmetric to the middle section of the buildings in idealized urban roughness layer when free wind flows perpendicularly to the street [17]. The boundary conditions in the lateral

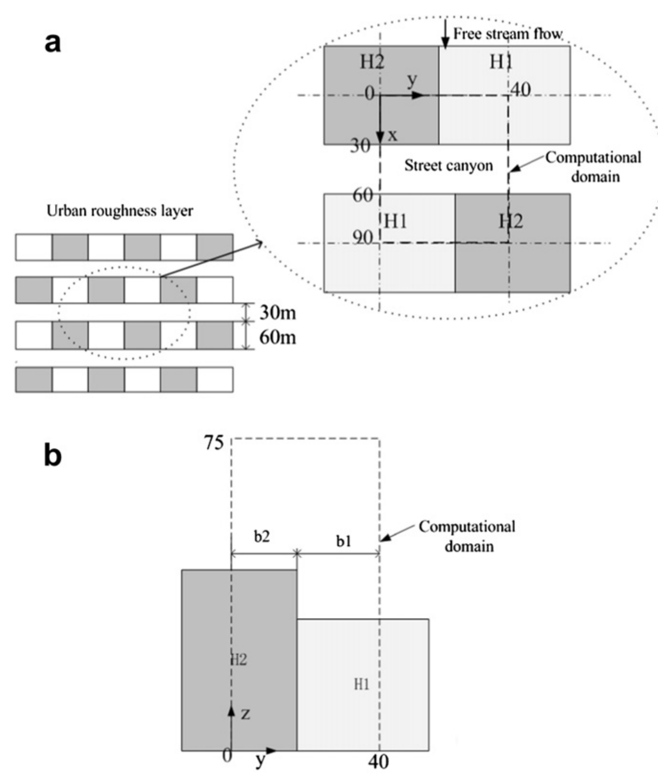

Fig. 1. Layout of non-uniform street canyon, in top view (a) and side view (b). The area depicted with dashed lines is the computational domain. Deep gray areas indicate the high buildings. H_1 and H_2 are the heights of the high building and low building, respectively. b_1 and b_2 are the lengths of the low and high buildings occupied in the computational domain, respectively.

direction are assumed symmetric as well. It should be pointed out that, the reasons for the symmetric boundary condition in the lateral direction are that the free boundary-layer air flows perpendicularly to the street canyon and buildings in the urban roughness layer are assumed in idealized layouts as shown in Fig. 1. The length of the computational domain in the lateral direction is $L = 40$ m. That in the longitudinal direction, x, is 90 m, which is three times of the street width ($W = 30$ m). Similar computational domains were used in many former studies [23–25]. A modified periodic boundary condition in the longitudinal direction is specified in the simulation as well, which will be described in Section 3.3. The computational domain in the vertical direction, z, is 2.5 times of H_1 (about $1.7H_2$). As is commonly known, the interface region between the canyon structure and the free shear region will extend above the buildings as thick as twice the building heights [17,26]. However, the vertical size of the computational domain is usually set two times of the building height under the periodic boundary wind conditions [27,28]. The periodic boundary wind conditions allow a realistic flow profile to develop in areas above the building roof level, which is not constrained by initial flow profile [23]. Generally, the computational domain is designed to involve the LES simulated large-scale vortices with sizes similar to the street width (W). The computational domain in the current work should be reasonable.

The layouts of non-uniform street canyons with stepup and/or stepdown notches are identified by the occupying ratio of high buildings (ORHB) in the computational domain along the street and their bilateral allocation of buildings as well as the combinations of stepup and/or stepdown notches. The high buildings on both street sides in the computational domain occupy the same areas along the street. As is shown in Fig. 1(b), b_1 is the length of a low building occupied in the computational domain and b_2 is the length of a high building occupied in the computational domain; the length of the computational domain in the lateral direction is $L = b_1+b_2 = 40$ m. Four cases are simulated with four combinations of b_1 and b_2 (see Fig. 2).

Case 1: $b_1 = 40$ m and $b_2 = 0$. The buildings on both sides of the street have the same height H_1. This case demonstrates the uniform street canyon.
Case 2: $b_1 = 30$ m and $b_2 = 10$ m, with low ORHB (0.25) and separate stepup and stepdown notches from each other, with opposite uniform low buildings in the middle.
Case 3: $b_1 = b_2 = 20$ m, with moderate ORHB (0.5) and adjoining stepup and stepdown notches.
Case 4: $b_1 = 10$ m and $b_2 = 30$ m, with larger ORHB (0.75) and separate stepup and stepdown notches from each other, but different from Case 2, here in the middle is part of the opposite uniform high buildings.

3. Mathematical equations and algorithms

3.1. Air flow equations

The large-eddy simulation (LES) method is widely used in solving the turbulence flow. In LES, large-scale vortices are calculated by solving the Navier–Stokes equations directly, only small scale vortices are modeled by subgrid stress (SGS) model. By applying the top-hat (box) filter to Navier–Stokes equations, the governing equations for LES are obtained in the form of continuity equation

$$\frac{\partial \overline{u_i}}{\partial x_i} = 0, \tag{1}$$

and the momentum equations

$$\frac{\partial \overline{u_i}}{\partial t} + \frac{\partial\left(\overline{u_i u_j}\right)}{\partial x_i} = -\frac{\partial \overline{p}}{\partial x_i} - \frac{\partial \tau_{ij}}{\partial x_j} + \frac{1}{\mathrm{Re}}\frac{\partial^2 \overline{u_i}}{\partial x_j \partial x_j}, \tag{2}$$

where $\overline{u_i}$ and $\overline{u_j}$ are the resolved-scale velocities in i and j directions, $\overline{p}$ is the resolved-scale virtual pressure, τ_{ij} is the SGS, which should be modeled. The modified and improved Smagorinsky SGS scheme [29] by using Qiu et al.'s [30] method to compute the characteristic length dynamically is used. The SGS terms in the governing equations can be parameterized as

$$\tau_{ij} = -2\nu_{\mathrm{sgs}}\overline{S}_{ij} + \frac{1}{3}\tau_{kk}\delta_{ij}, \tag{3}$$

in which

$$\nu_{\mathrm{sgs}} = C_s^2 l_{\mathrm{sgs}}^2 |\overline{S}|. \tag{4}$$

$\overline{S}_{ij}$ is the resolved strain-rate tensor. C_s is the Smagorinsky model constant ($C_s = 0.08$), ν_{sgs} is the subgrid viscosity, and l_{sgs} is the subgrid characteristic length. The subgrid viscosity varies in different eddy viscosity SGS models. In the initial Smagorinsky model [29], the grid width instead of the characteristic length of SGS motions is used. However, the grid width is a geometrical length scale that depends on the actual implementation of LES. Spatial heterogeneities of SGS motions lead to spatial differences of the subgrid characteristic length of SGS motions, which cannot be reflected by a fixed grid width. Here, we compute the subgrid characteristic length self-adaptively. For details about the calculation of l_{sgs}, please refer to Qiu et al. [30].

3.2. Scalar pollutant transport equation

Pollutant dispersions in street canyons are investigated by solving the scalar transport equation

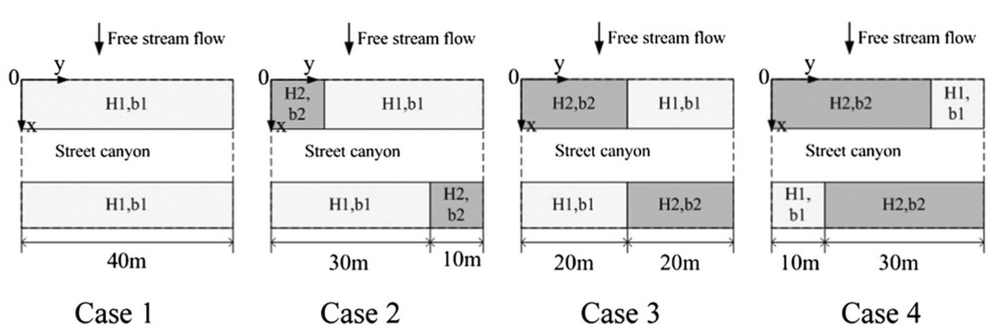

Fig. 2. Four cases of street building layouts.

$$\frac{\partial \overline{c}}{\partial t} + \frac{\partial (\overline{u_i c})}{\partial x_i} = -\frac{\partial \sigma_i}{\partial x_i} + \frac{1}{ReSc}\frac{\partial^2 \overline{c}}{\partial x_i \partial x_i} + S_0, \tag{5}$$

in which

$$\sigma_i = -\nu_c \frac{\partial \overline{c}}{\partial x_i}. \tag{6}$$

$\overline{c}$ is the resolved-scale scalar mixing ratio, Sc is the Schmidt number ($Sc = 1$), S_0 is the emission source, and σ_i is SGS turbulent diffusion. ν_c is calculated by $\nu_c = \nu_{sgs}/S_c$.

3.3. Boundary conditions and algorithms

A uniform grid system with the spatial resolution of 1 m is used. Inlet-and-outlet boundaries in the longitudinal direction are set to be symmetrically periodic conditions as follows:

$$\overline{u}_{i,\mathrm{inlet},L/2\pm\Delta y,z} \leftrightarrow \overline{u}_{i,\mathrm{outlet},L/2\mp\Delta y,z}, \tag{7}$$

where i range (1, 2, 3) presents the wind velocity in (x, y, z) directions, Δy means the distance from the grid point to the middle plane in the lateral direction. The top boundary is under the slip condition with zero vertical gradients. Non-slip wall conditions are used at all solid walls. Wall functions are used to modify the velocities on the nearest grid points to the wall [31].

A line source located at the center of the canyon is used to represent the vehicle emissions.

In the current work, we consider the case when ambient free stream air flow transverse to the street canyon in the positive direction of the x-axis (see Fig. 1). The initial value of the free stream wind profile above the urban roughness layer is similar to what Baik and Kim used [32] and is given by

$$u = U_{\mathrm{ref}}\left(\frac{z - H_1}{z_{\mathrm{ref}}}\right)^{0.299}, \tag{8}$$

where U_{ref}, which is set to be 1 m s^{-1}, is the reference wind velocity at the reference height $z_{\mathrm{ref}} = 2$ m above the low building height. The initial wind profile has no obvious effect on the ultimate wind profile inside and above the street canyon, as shown by Cui et al. [28].

In simulation of air flow inside and above street canyons, the Reynolds number ($Re = U_{\mathrm{ref}} \cdot H_1/\nu$) is usually scaled down so as to resolve the flow turbulence sufficiently with extensive grid systems and to reduce the computational load [24,33]. However, to obtain the air flow structure Re independence, the Re should be larger than the critical value. Some papers refer the critical Re as 3400 [34,35], but other paper refer it much larger as 1.1×10^4 [36]. In this work, the Re is set to be 1.2×10^4 artificially.

The resolved-scale dynamic equations of the mathematical model are solved by the Finite Volume Method (FVM), with the SIMPLE algorithm [37] used to deal with the implicit dependence of velocity and pressure. Self-developed software is used that has been validated in reference [14]. The time steps are set to be 0.02s in all the simulations.

4. Results and discussions

Statistical averages on wind velocities and pollutant concentrations are collected for 200 s after the flow has fully developed. Hereafter, statistically-averaged results are shown, and the wind velocity amplification and the "wall effect" induced by high buildings are discussed.

4.1. Air flow structures

Air flow structure is one of the primary concerns in analyzing the effect of uneven building layout on air flow and pollutant dispersion in street canyons. Wind velocity amplification and wind direction change can induce the change of pollutant dispersion characteristics inside and above street canyons. The air flow structure and wind velocity distributions in the street canyon of our uniform case (Case 1) will be shown first, for model validation. Then, air flow structures in the non-uniform cases are analyzed.

4.1.1. Uniform street canyon case

Fig. 3(a–c) show the vertical profiles of the velocity (u) in longitudinal direction inside and above the street canyon in Case 1, with the horizontal coordinates (x, y) to be (37.5 m, 20 m), (45 m, 20 m), and (52.5 m, 20 m), respectively, in the middle cross section. The simulated wind velocities in this work (with $Re = 1.2 \times 10^4$) are compared with the large-eddy simulations conducted by Liu et al.

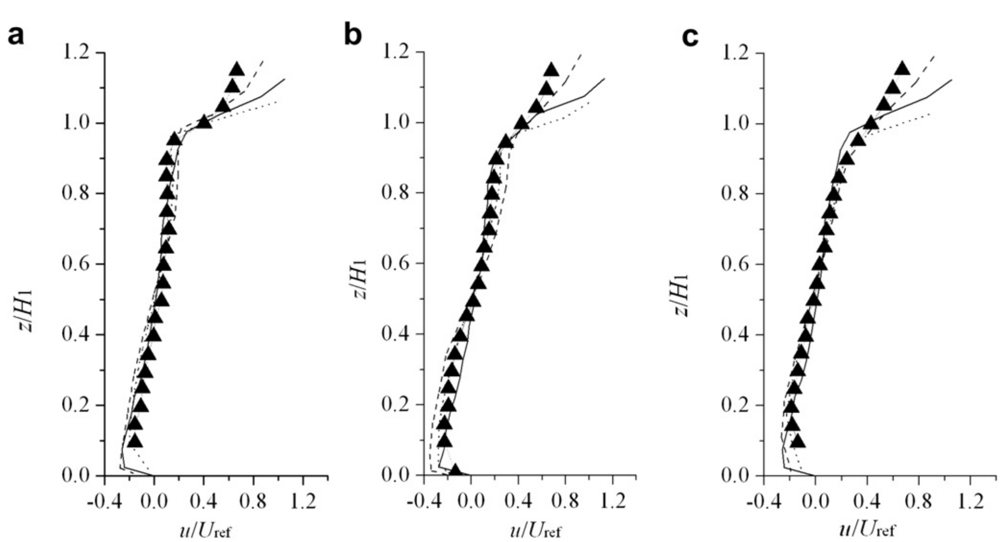

Fig. 3. Comparisons of 3 vertical profiles of the longitudinal direction velocity component, u, inside and above the uniform street canyon in Case 1, with the horizontal coordinates to be (37.5 m, 20 m) (Fig. (a)), (45 m, 20 m) (Fig. (b)) and (52.5 m, 20 m) (Fig. (c)), respectively, in the middle cross section. Straight line indicates the current simulation, dashed line denotes the LES results from Cui et al., dot line gives the LES results from Liu et al., and diamond shows the physical model measurements from Li et al.

(with $Re = 1.2 \times 10^4$) [38] and Cui et al. (with $Re = 1.5 \times 10^6$) [28] and the physical model measurements conducted by Li et al. (with $Re = 1.2 \times 10^4$) [39], among which the real Re was used by Cui et al. in their LES. It is shown that all these works produce very similar wind profiles inside the canyons, with slight difference near the road surfaces and the roofs and considerable difference above the street canyons. The remarkable difference of the wind profiles above the street canyons might result from the difference of initial wind profile and boundary conditions, while the slight difference inside the canyons might be caused by different grid spatial resolutions and wall treatments. However, these results prove that the scaling down of the Re in the current simulation has no obvious influence on the simulation results. All the simulations and physical model measurements show a primary vortex inside the canyon as shown in Fig. 4(a) and (b) shows the horizontal air flow structure inside the street canyon at $z = 2$ m from the ground, where the air mass flow from the windward wall to the leeward wall and wind vectors are relatively regular. The results, as shown in Figs. 3 and 4, verify the promise of the current simulation on air flow structure inside and above the street canyon.

4.1.2. Non-uniform street canyon cases

The flow fields depicted by vectors in Case 2 are shown in Fig. 5(a–f). The flow patterns here are more complicated than those in Case 1. The velocity vectors are significantly amplified, particularly in the vicinity of the high buildings. Hu and Wang [17] have shown that a single high-rise building can cause sudden amplification of wind velocity in its vicinity. In Case 2, the air flow is separated at the top area of the high building wall in the stepup section, forming a strong down washing (see Fig. 5(b, d)). In the stepdown section, low pressure is engendered behind the upwind high building, which attracts the air mass in the strong down washing and causes the wind near the road surface tilting to the upwind high building (Fig. 5(e)). It also results in amplification of the upwind velocity behind the upwind high building (Fig. 5(a, c)), and the air flow re-circulations in the stepup and stepdown notches are not clear (Fig. 5(a, b)). These air flow structures are obviously different from the results of the simulated and physical model experiment conducted by Baik et al. [6], where only the stepup (or stepdown) notch flow was studied in one of the simulations. These different flow patterns illustrate the effects of uneven building layouts on the air flow in the non-uniform street canyons. Fig. 5(e) also demonstrates the existence of the horizontal divergence of air flow in front of the downwind high building and the horizontal convergence of air flow behind the upwind high building. The existence of horizontal divergence of air flow in a non-uniform street canyon was shown by Nelson et al. [19] in their in-situ measurements.

Fig. 6 shows a stream line in Case 2, which clearly illustrates the wind flow structures in the non-uniform street canyon. Spiral circulations dominate the air flow inside the street canyon, and it can be clearly seen that the wind direction tilts near the leeward wall, near the windward wall and near the road surface (Fig. 5(c–e)). The air flows on the top of the upwind low building which go down to the street canyon experience several re-circulations and eventually go

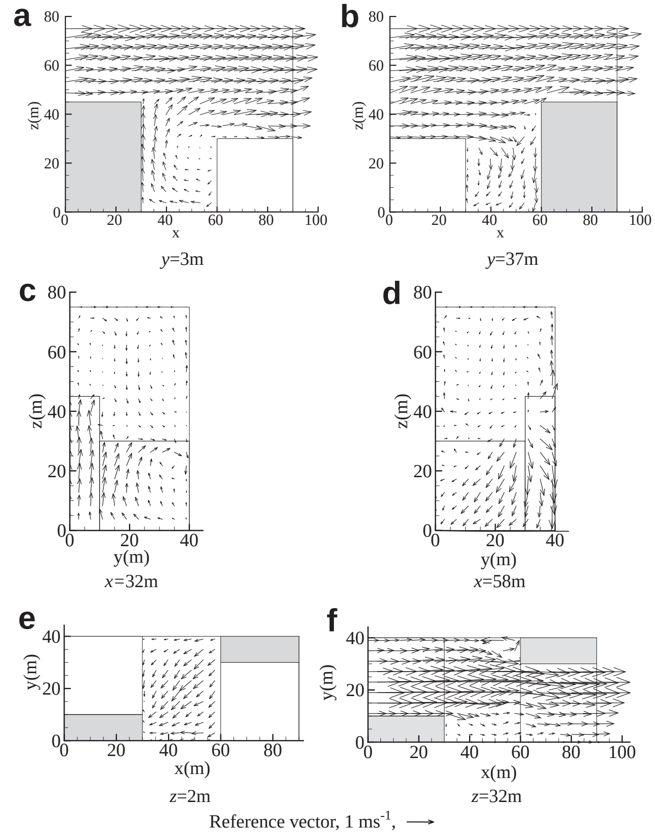

Fig. 5. The velocity vectors in (a) the longitudinal vertical plane in the stepdown section, $y = 3$ m, (b) the longitudinal vertical plane in the stepup section, $y = 37$ m, (c) the lateral vertical plane at 2 m from the leeward wall, $x = 32$ m, (d) the lateral vertical plane at 2 m from the windward wall, $x = 58$ m, (e) the horizontal plane near road surface, $z = 2$ m, (f) the horizontal plane 2 m over lower building top, $z = 32$ m for Case 2.

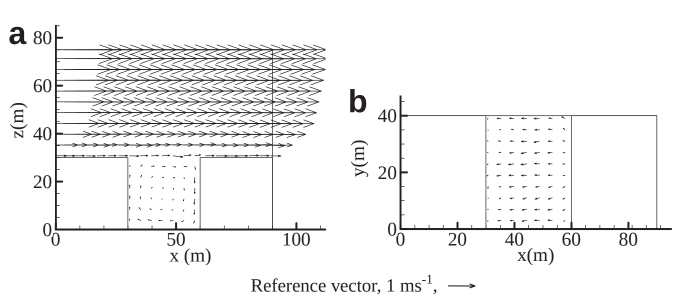

Fig. 4. (a) The velocity vectors in the longitudinal vertical plane at $y = 20$ m for Case 1, (b) the velocity vectors in the horizontal plane at $z = 2$ m for Case 1.

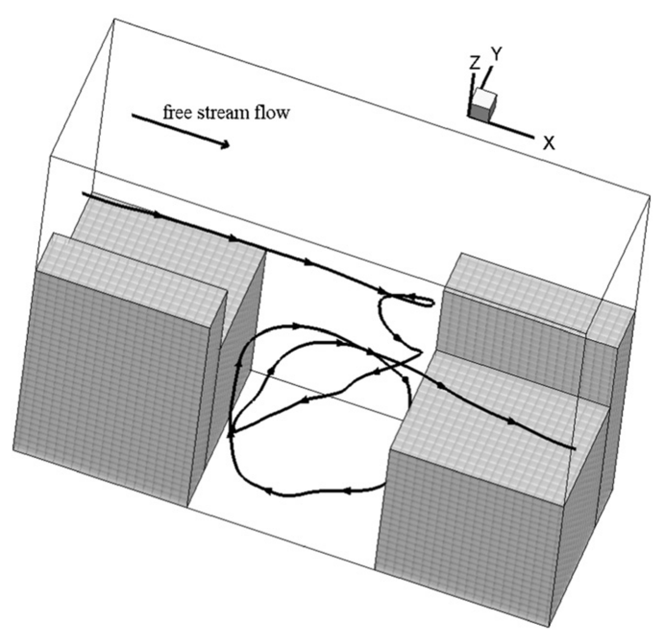

Fig. 6. A typical stream line in the non-uniform street canyon of Case 2.

out of the canyon over the top of the downwind low building. This air flow feature reveals that there are large-scale air exchanges of air mass inside and above the non-uniform street canyons.

Fig. 7(a–f) and Fig. 8(a–f) illustrate the flow fields depicted by vectors in Case 3 and Case 4, respectively.

In Case 3, the flow structures near the leeward wall, the windward wall and the road surface are more complicated compared to those in Case 2, and there are no distinct horizontal divergence of air flow in front of the downwind high building or horizontal convergence of air flow behind the upwind high building (see Fig. 7(c–e)). The air streamlines near the windward wall, as shown in Fig. 7(d), tilt in the region higher than H_1, leading to the circle flow in horizontal plane around the high buildings and the vortices behind the upwind high building and beside the downwind high building (see Fig. 7(f)). These vortices increase the air stagnating around the high buildings and decrease the wind velocities inside and above the street canyon. In Case 3, the wind velocities above low buildings are lower than those in Case 2, as illustrated in Fig. 5(a, b) and Fig. 7(a, b). The reasons might be the increase of obstructing of air flow resulted from the high-density high buildings.

Similar to those in Case 2, the air streamlines in Case 4 tilt distinctly near the leeward wall, the windward wall and the road surface (Fig. 8(c, d)), resulting in wind velocity amplifications in the vicinity of the high buildings (Fig. 8(a–f)). The horizontal divergence of air flow in front of the downwind high building and the horizontal convergence of air flow behind the upwind high building are found near the road surface in Case 4, just like those in Case 2.

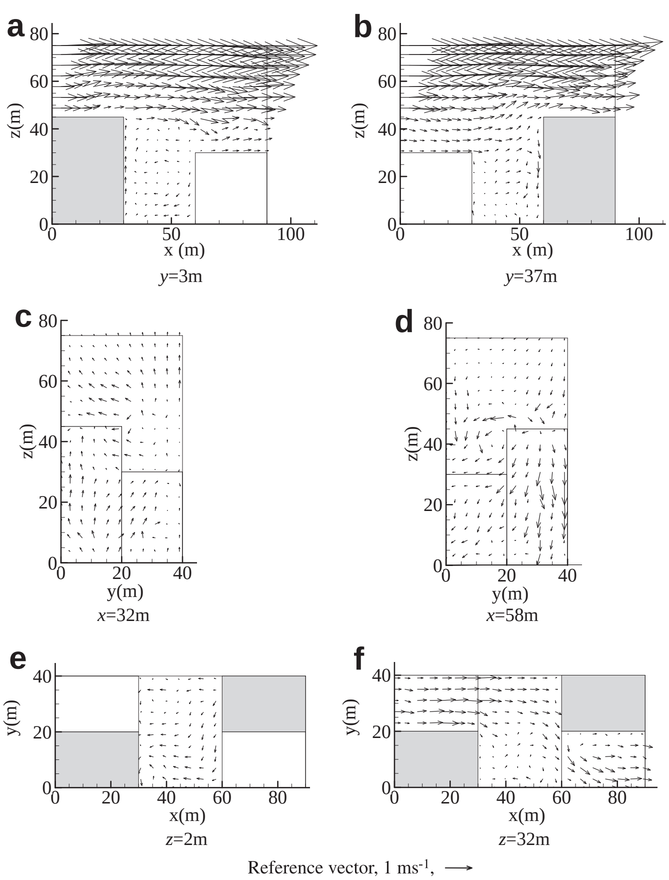

Fig. 7. The velocity vectors in (a) the longitudinal vertical plane in the stepdown section, $y = 3$ m, (b) the longitudinal vertical plane in the stepup section, $y = 37$ m, (c) the lateral vertical plane at 2 m from the leeward wall, $x = 32$ m, (d) the lateral vertical plane at 2 m from the windward wall, $x = 58$ m, (e) the horizontal plane near road surface, $z = 2$ m, (f) the horizontal plane 2 m over lower building top, $z = 32$ m for Case 3.

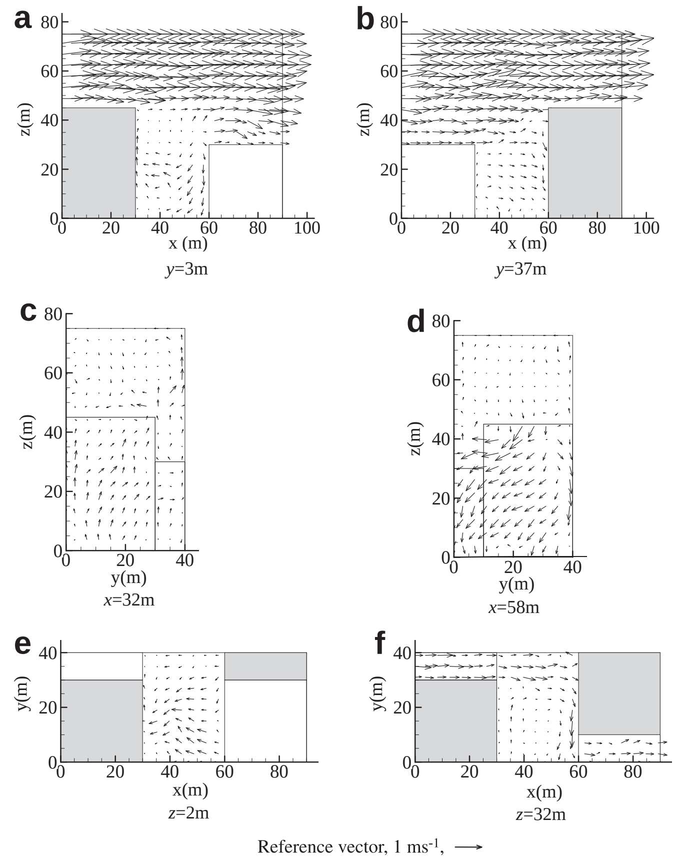

Fig. 8. The velocity vectors in (a) the longitudinal vertical plane in the stepdown section, $y = 3$ m, (b) the longitudinal vertical plane in the stepup section, $y = 37$ m, (c) the lateral vertical plane at 2 m from the leeward wall, $x = 32$ m, (d) the lateral vertical plane at 2 m from the windward wall, $x = 58$ m, (e) the horizontal plane near road surface, $z = 2$ m, (f) the horizontal plane 2 m over lower building top, $z = 32$ m for Case 4.

In general, the flow patterns in Case 2 and Case 4 are similar, but different from that in Case 3. The reason is that the separating of stepup notch and stepdown notch along the street in Case 2 as well as in Case 4 causes the tilting of air flow streamlines and the amplification of wind velocities inside and above the street canyon, while the adjoining of stepup notch and stepdown notch in Case 3 increases the air stagnating around the high buildings and decreases the wind velocities inside and above the street canyon.

4.2. Mean wind profiles

It is well known that building obstacles in urban roughness layer can break down the wind flow and change the wind profile, making the air flow different from that in rural boundary-layer [40,41]. Fig. 9 shows the averaged velocity u at the horizontal coordinate, (45 m, 20 m).

In Case 2, the occupying ratio of the unilateral high building along the street is low, and the stepup notch is apart from the stepdown notch, with opposite part of uniform low buildings in the middle. The simulated wind profile in Case 2 demonstrates two obvious shear layers: one is near the ground and the other is near the height of the low building. The latter shear layer is similar to that in the uniform street canyon in Case 1 with the building height H_1, but the shear rate is greater. However, the wind velocities are considerably increased inside and above the street canyon in Case 2 than those in Case 1, demonstrating the wall effect of high buildings that increases wind velocities in their vicinities.

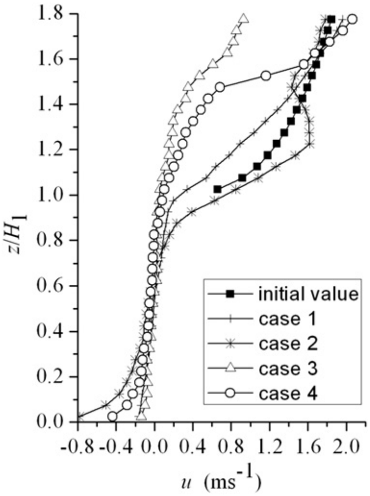

Fig. 9. The mean wind profiles in the four cases and the initial wind velocity values inside and above the street canyons. ■ – the initial value, + – the simulated results in Case 1, * – the simulated results in Case 2, Δ – the simulated results in Case 3, and ○ – the simulated results in Case 4.

In case 4, the unilateral high building along the street has a high occupying ratio, and the stepup notch separate from the stepdown notch, with part of opposite uniform high buildings in the middle. The wind profile in Case 4 demonstrates two obvious shear layers: one near the ground and the other near the height of the high building. The shear layer near the height of the high building is similar to that in the uniform deep street canyon with the building height H_2, but with a greater shear rate. The wind velocities inside the street canyon, at a level lower than the low building, are greater than those in the uniform street canyon in Case 1. This indicates that, when the occupying ration of high buildings is high, the obstructing of air flow becomes more evident and thus increases the wind velocities in the vicinities of the high buildings in non-uniform street canyons.

In Case 3, the occupying ratio of the high buildings is moderate, and the stepup notch is adjoining to the stepdown notch. The simulated wind velocities inside and above the street canyon are lower than those in either Case 2 or Case 4, and even lower than those in Case 1. It follows that the wall effect of high buildings in Case 3 is enough to decrease the wind velocities in urban roughness layer. The simulated wind profile in this case is similar to those inside and above a staggered obstacle array, where the air flows circle around high buildings and the shear layer above the obstacles is usually weak [42,43]. The differences of wind profiles among Cases 3, 2 and 4 indicate that obstacle arrays in street canyons have evident effects on air flows in urban roughness layer.

4.3. Pollutant distributions and dispersions

Pollutant concentrations are normalized by

$$C^* = \frac{C \cdot U_{\mathrm{ref}} \cdot H_1}{Q/L}, \tag{9}$$

where C^* is the normalized pollutant concentration, C is the resolved pollutant concentration, U_{ref} is the reference wind velocity, Q is the pollutant emission rate (in $\mu g.s^{-1}$), and L is the street length in the computational domain.

The simulated pollutant concentrations of the three kinds of non-uniform street canyons are illustrated in Fig. 10(a–f). Fig. 10(a, c, e) are the contours of pollutant concentrations in the lateral vertical plane at $x = 32$ m (2 m from the leeward wall), and Fig. 10(b, d, f) are those in the horizontal plane at the pedestrian level 1.5 m from the road surface, respectively. Compared to the pollutant distribution in the uniform street canyon, where pollutants emitted from vehicles are transported to the leeward wall and then to the top areas along the leeward wall, the pollutant concentration in the

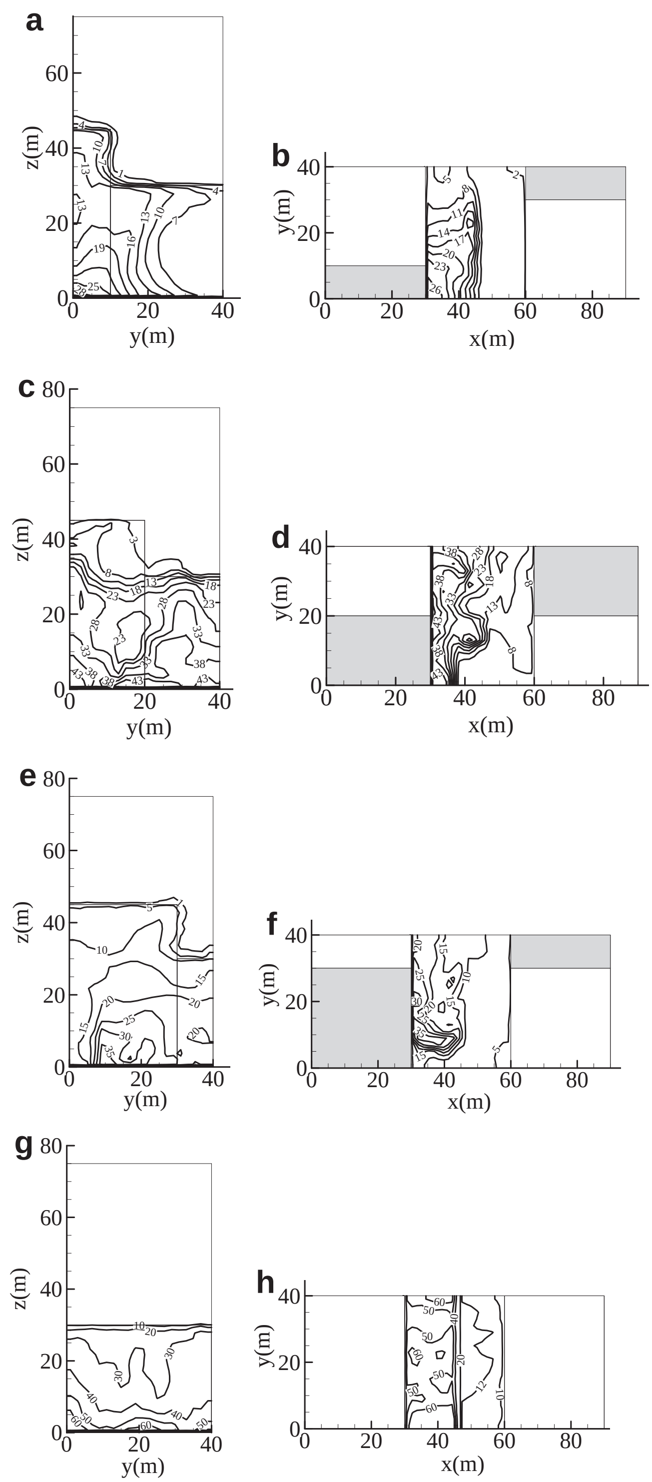

Fig. 10. Contours of the simulated normalized pollutant concentrations in different cases of non-uniform street canyons in planes 2 m from the leeward walls ((a), (c), (e), (g)) and at the pedestrian level 1.5 m above the road surface ((b), (d), (f), (h)). Figs. (a) and (b) are the simulated results of Case 2, (c) and (d) are the simulated results of Case 3, (e) and (f) are the simulated results of Case 4, (g) and (h) are the simulated results for the uniform street canyon Case 1.

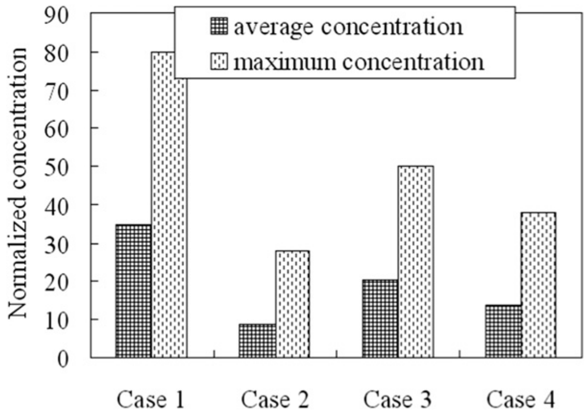

Fig. 11. The average and maximum normalized concentrations at the pedestrian level of four cases.

non-uniform street canyons has an evident non-uniform distribution, affected by the non-uniform wind field (Fig. 10(a–f)). In Case 2 and Case 4 (Fig. 10(a, b, e, f)), after pollutants are transported to the leeward wall, the lateral accumulation of pollutants occurs behind the upwind high building due to the horizontal convergence of air flow (see Fig. 5(e) and Fig. 8(e)). In Case 3 (Fig. 10(c, d)), there is no lateral accumulation of pollutants near the leeward wall along the street, for there is no distinct horizontal convergence of air flow (see Fig. 7(e)).

The mean and maximum normalized pollutant concentrations at the pedestrian level (1.5 m above the road surface) in the four cases are compared in Fig. 11. Case 1 has the extremes of the mean and maximum concentrations, followed by Cases 3, 4 and then 2. These results reveal that in the non-uniform street canyons, the uneven building layouts can enhance pollutant dispersions since there existing large-scale air exchanges of air mass inside and above such canyons. For different uneven building layouts in non-uniform street canyons, the mean pollutant concentrations in Cases 2 and 4 are lower than that in Case 3, suggesting that the separating of stepup and stepdown notches along the street canyon might be a good choice for uneven building layouts, from the point of view of pollutant dispersion.

Although the designed non-uniform building layouts presented the characteristics of actual street canyons, they are still different from real ones. Especially the gaps between adjacent buildings along the real streets are ignored in the current street canyon models. Simulations of street-level winds in a building array carried out by Hu et al. [17] show the horizontal air flow inside the street canyons may be disturbed by the cross wind in these gapes, which may result in the shifting of the horizontal convergence of air flow to the windward wall. Further studies are in need in order to achieve more universal results.

5. Conclusions

In actual street canyons, buildings along streets usually present uneven layouts. Air flow patterns inside the street canyons are significantly affected by the building layouts. To investigate the effects of non-uniform street canyon layouts on air flow, alternative layouts of different high buildings are designed for modeling simplified non-uniform street canyons, in which the relative locations of the opposite buildings produce different combinations of stepup and/or stepdown notches.

The simulated results show more complicated air flow structures in non-uniform street canyons than those in uniform street canyons. Some new street canyon flow features, such as wind streamlines tilting, horizontal divergence and convergence of air flow and large-scale air exchanges of air mass inside and above the street canyons are found in non-uniform street canyons. The separation of stepup notch and stepdown notch along the street canyon for uneven building layouts increases the wind velocities in the vicinity of high buildings, while the adjoining of the notches decreases the wind velocities and results in no distinct horizontal divergence of air flow in front of the downwind high building and horizontal convergence of air flow behind the upwind high building.

The simulations of pollutant concentrations in three cases of non-uniform street canyons demonstrate that the pollutant concentration in the non-uniform street canyons has an evidently uneven distribution arising from the non-uniform wind field. It is found that the uniform street canyon has the extreme of mean and maximum normalized pollutant concentrations. These results reveal that uneven street building layouts can enhance pollutant dispersions since there existing large-scale air exchanges of air mass inside and above such non-uniform street canyons. For non-uniform street canyons, the separation of stepup notch and stepdown notches should be a better choice for uneven building layout, from the point of view of pollutant dispersion.

Although the designed non-uniform building layouts presented the characteristics of actual street canyons, they are still different from real ones. Further studies are in need in order to achieve more universal results.

Acknowledgments

This study is financially supported by the National Natural Science Foundation of China (No. 10872159), Interdisciplinary Programs of Xi'an Jiaotong University (2009xjtujc10). It is also supported by Hong Kong Polytechnic University (G-YX3L and GU-481).

References

[1] Depaul FT, Sheih CM. Measurements of wind velocities in a street canyon. Atmospheric Environment 1986;20(3):455–9.
[2] Oke TR. Street design and urban canopy layer climate. Energy and Building 1988;11:103–13.
[3] Xie XM, Huang Z, Wang JS, Xie Z. The impact of solar radiation and street layout on pollutant dispersion in street canyon. Building and Environment 2005;40(2):201–12.
[4] Niachou K, Livada I, Santamouris M. Experimental study of temperature and airflow distribution inside an urban street canyon during hot summer weather conditions. Part II: airflow analysis. Building and Environment 2008; 43(8):1393–403.
[5] Hang J, Li Y, Sandberg M, Claesson L. Wind conditions and ventilation in high-rise long street models. Building and Environment 2010;45(6):1353–65.
[6] Baik JJ, Park RS, Chun HY, Kim JJ. A laboratory model of urban street-canyon flows. Journal of Applied Meteorology 2000;39(9):1592–600.
[7] Ahmad K, Khare M, Chaudhry KK. Wind tunnel simulation studies on dispersion at urban street canyons and intersections—a review. Journal of Wind Engineering and Industrial Aerodynamics 2005;93(9):697–717.
[8] Kastner-Klein P, Rotach MW. Mean flow and turbulence characteristics in urban roughness sublayer. Boundary-Layer Meteorology 2004;111:55–84.
[9] Gromke C, Ruck B. On the impact of trees on dispersion processes of traffic emissions in street canyons. Boundary-Layer Meteorology 2009;131(1):19–34.
[10] Kumar P, Garmory A, Ketzel M, Berkowicz R, Britter R. Comparative study of measured and modelled number concentrations of nanoparticles in an urban street canyon. Atmospheric Environment 2009;43(4):949–58.
[11] Li XL, Wang JS, Tu XD, Liu W, Huang Z. Vertical variations of particle number concentration and size distribution in a street canyon in Shanghai, China. Science of the Total Environment 2007;378(3):306–16.
[12] Yang Y, Shao Y. Numerical simulations of flow and pollutant dispersion in urban atmospheric boundary layers. Environmental Modeling & Assessment 2008;23:906–21.
[13] Murena F, Favale G, Vardoulakis S, Solazzo E. Modelling dispersion of traffic pollution in a deep street canyon: application of CFD and operational models. Atmospheric Environment 2009;43(14):2303–11.
[14] Gu ZL, Zhang YW, Lei KB. Large eddy simulation of flow in a street canyon with tree planting under various atmospheric instability conditions. SCIENCE CHINA Technological Sciences 2010;53(7):1928–37.

[15] Balczo M, Gromke C, Ruck B. Numerical modeling of flow and pollutant dispersion in street canyons with tree planting. Meteorologische Zeitschrift 2009;18(2):197–206.
[16] Nelson MA, Pardyjak ER, Brown MJ, Klewicki JC. Properties of the wind field within the Oklahoma City Park Avenue street canyon. Part II: spectra, cospectra, and quadrant analyses. Journal of Applied Meteorology and Climatology 2007;46(12):2055–73.
[17] Hu CH, Wang F. Using a CFD approach for the study of street-level winds in a built-up area. Building and Environment 2005;40(5):617–31.
[18] Yim SHL, Fung JCH, Lau AKH, Kot SC. Air ventilation impacts of the “wall effect” resulting from the alignment of high-rise buildings. Atmospheric Environment 2009;43(32):4982–94.
[19] Nelson MA, Pardyjak ER, Klewicki JC, Pol SU, Brown MJ. Properties of the wind field within the Oklahoma City Park Avenue street canyon. Part I: mean flow and turbulence statistics. Journal of Applied Meteorology and Climatology 2007;46(12):2038–54.
[20] Meroney RN, Pavageau M, Rafailidis S, Schatzmann M. Study of line source characteristics for 2-D physical modelling of pollutant dispersion in street canyons. Journal of Wind Engineering and Industrial Aerodynamics 1996;62:37–56.
[21] Liu CH, Cheng WC, Leung TCY, Leung DYC. On the mechanism of air pollutant re-entrainment in two-dimensional idealized street canyons. Atmospheric Environment 2010, doi:10.1016/j.atmosenv.2010.03.015.
[22] Gromke C, Buccolieri R, Di Sabatino S, Ruck B. Dispersion study in a street canyon with tree planting by means of wind tunnel and numerical investigations – evaluation of CFD data with experimental data. Atmospheric Environment 2008;42(37):8640–50.
[23] Walton A, Cheng AYS. Large-eddy simulation of pollution dispersion in an urban street canyon – part II: idealised canyon simulation. Atmospheric Environment 2002;36(22):3615–27.
[24] Liu CH, Leung DYC, Barth MC. On the prediction of air and pollutant exchange rates in street canyons of different aspect ratios using large-eddy simulation. Atmospheric Environment 2005;39(9):1567–74.
[25] Zhang YW, Gu ZL, Cheng Y, Lee SC. Effect of real-time boundary wind conditions on the air flow and pollutant dispersion in an urban street canyon–large eddy simulations. Atmospheric Environment 2011;45(20):3352–9.
[26] Flowe AC, Kumar A. Analysis of velocity fields and dispersive cavity parameters as a function of building width to building height ratio using a 3-D computer model for squat buildings. Journal of Wind Engineering and Industrial Aerodynamics 2000;86(2–3):87–122.
[27] Li XX, Liu CH, Leung DYC. Large-eddy simulation of flow and pollutant dispersion in High-aspect-ratio urban street canyons with wall model. Boundary-Layer Meteorology 2008;129:249–68.
[28] Cui ZQ, Cai XM, Baker CJ. Large-eddy simulation of turbulent flow in a street canyon. Quarterly Journal of the Royal Meteorological Society 2004;130(599):1373–94.
[29] Smagorinsky J. General circulation experiments with the primitive equations: part 1. The basic experiment. Monthly Weather Riview 1963;91:99–164.
[30] Qiu J, Gu ZL, Wang ZS. Numerical study of the response of an atmospheric surface layer to a spatially nonuniform plant canopy. Boundary-Layer Meteorology 2008;127:293–311.
[31] Walton A, Cheng AYS, Yeung WC. Large-eddy simulation of pollution dispersion in an urban street canyon – part I: comparison with field data. Atmospheric Environment 2002;36(22):3601–13.
[32] Baik JJ, Kim JJ. A numerical study of flow and pollutant dispersion characteristics in urban street canyons. Journal of Applied Meteorology 1999;38(11):1576–89.
[33] Uehara K, Wakamatu S, Ooka R. Studies on critical Reynolds number indices for wind-tunnel experiments on flow within urban area. Boundary-Layer Meteorology 2003;107:353–70.
[34] Pavageau M, Schatzmann M. Wind tunnel measurements of concentration fluctuations in an urban street canyon. Atmospheric Environment 1999;33(24–25):3961–71.
[35] Hoydysh WG, Griffiths RA, Ogawa Y. A scale model study of the dispersion of pollutant in street canyons. In: the 67th annual meeting of the air pollution control association. Denver, CO; 1974. p. 1–13.
[36] Snyder WH. Similarity criteria for the application of fluid models to the study of air pollution meteorology. Boundary-Layer Meteorology 1972;3(1):113–34.
[37] Tao WQ. Recent advancement in numerical heat transfer. Bei Jing: Science Press; 2005.
[38] Liu CH, Barth MC, Leung DYC. Large-Eddy simulation of flow and pollutant transport in street canyons of different building-height-to-street-width ratios. Journal of Applied Meteorology 2004;43(10):1410–24.
[39] Li XX, Liu CH, Leung DYC, Lam KM. Physical modeling of flow field inside urban street canyons. Journal of Applied Meteorology and Climatology 2008;41:2058–67.
[40] Dupont E, Menut L, Carissimo B, Pelon J, Flamant P. Comparison between the atmospheric boundary layer in Paris and its rural suburbs during the ECLAP experiment. Atmospheric Environment 1999;33(6):979–94.
[41] Rotach MW, Vogt R, Bernhofer C, Batchvarova E, Christen A, Clappier A, et al. BUBBLE – an urban boundary layer meteorology Project. Theoretical and Applied Climatology 2005;81(3):231–61.
[42] Davidson MJ, Snyder WH, Lawson RE, Hunt JCR. Wind tunnel simulations of plume dispersion through groups of obstacles. Atmospheric Environment 1996;30(22):3715–31.
[43] Shi RF, Cui GX, Wang ZS, Xu CX, Zhang ZS. Large eddy simulation of wind field and plume dispersion in building array. Atmospheric Environment 2008;42(6):1083–97.